Materials Science and Engineering A 506 (2009) 125–129

Contents lists available at ScienceDirect

Materials Science and Engineering A

journal homepage: www.elsevier.com/locate/msea

Mechanical behaviour characterisation of silicon and effect of loading rate on pop-in: A nanoindentation study under ultra-low loads

Li Chang, Liangchi Zhang*

School of Aerospace, Mechanical and Mechatronic Engineering, The University of Sydney, Sydney, NSW 2006, Australia

ARTICLE INFO

Article history:
Received 14 August 2008
Received in revised form
13 November 2008
Accepted 14 November 2008

Keywords:
Silicon
Nanoindentation
Young's modulus
Pop-in
Phase transformation

ABSTRACT

This paper aims to clarify the confusion in interpreting the deformation mechanism of monocrystalline silicon subjected to nanoindentation. The indentation tests were carried out over an ultra-low range of loads with various loading rates using a Berkovich indenter. It was found that with a proper area function of the indenter tip the mechanical properties of silicon can be accurately characterised, that a pop-in event may occur upon ultra-low loading and represents the onset of phase transition, and that a lower loading rate favors a sudden volume change but a rapid loading process tends to generate a gradual slope change of the load–displacement curve.

1. Introduction

Monocrystalline silicon is a key material in semiconductor industry, particularly in the development of micro/nano-electromechanical systems (MEMS/NEMS). To design and fabricate MEMS/NEMS, an in-depth understanding of the deformation mechanisms in silicon during surface processing is essentially required. However, the constitutive description of the material is still unavailable as its nanomechanical properties are not fully understood, which hinders the further development of new generations of high performance devices.

Over the past decade, the depth-sensing nanoindentation has been a focus of research to characterise the nanomechanical behaviour of silicon [1–4]. In particular, because the contact mode in nanoindentation is geometrically akin to that in ultra-precision machining, results from nanoindentation can provide valuable information for optimizing the machining conditions to achieve high surface finish with damage-free subsurface. However, the interpretation of nanoindentation results is not straightforward because the measurement is affected by many factors. For instance, the Young's modulus of silicon (1 0 0) reported ranges from 118 GPa to 190 GPa, depending on indentation depth [5,6]. As a result, various values of silicon modulus, e.g. 80 GPa [7], 168 GPa [8], and 200 GPa [9] have been used for theoretical and numerical analysis, leading to confusions in understanding the intrinsic mechanical behaviour of silicon. Another key issue in characterising the properties of monocrystalline silicon subjected to nanoindentaion is to explore the material's phase transformation mechanisms via the study on the load–displacement behaviour. It has been noticed that a distinct displacement discontinuity in loading, known as "pop-in", may occur under the indentation with spherical indenters [1,10–12]. Such pop-in discontinuity has been regarded as an important evidence of phase transformation from the cubic diamond Si-I to a metallic structure Si-II which was found to occur under hydrostatic loading in a diamond anvil cell experiment [11]. The 'interpretation' was due to the coincidence that the transformation from Si-I to Si-II causes a volume reduction [11], which could just be used to 'explain' discontinuity in the load–displacement curve of indentation. Accordingly, the location of a pop-in was assumed as a signal of the onset of the phase transition [1,10]. The assumption was supported by molecular dynamics analysis [13,14] and in situ measurement of the electrical resistance change in AFM indentation [15], which did show that β-tin appear during nanoindentation. However, the detailed microstructural change at pop-in has not been clearly understood. Some studies [4] suggested that a pop-in might simply be caused by a sudden extrusion of the transformed material as the phase transformation could have started at an earlier stage of loading. Some others [6] proposed that all the phase transformation, subsurface cracking, or sudden dislocation bursts may contribute to a pop-in. Nevertheless, recent investigations using sharp indenters [16,17] found that many surface cracks appeared after indentation while pop-ins occurred during indenta-

* Corresponding author. Tel.: +61 2 9351 2835.
E-mail address: l.zhang@usyd.edu.au (L. Zhang).

0921-5093/$ – see front matter © 2008 Elsevier B.V. All rights reserved.
doi:10.1016/j.msea.2008.11.021

tion, but that no dislocation was identified. These seem to indicate that phase transformations were initiated before dislocation nucleation and that a pop-in was independent of dislocations [17].

In the present work, the indentation tests were carried out under different loading conditions using a Berkovich indenter. The investigation tends to clarify two central issues in characterising the nanomechanical properties of silicon under nanoindentation: its Young's modulus and microstructural changes at pop-in. In particular, to reveal the origin of the pop-ins, nanoindentation tests were carried under ultra-low loads to avoid possible cracking and dislocation during an indentation [13,18].

2. Experiment

All experiments were performed on the (100) surface of monocrystalline silicon, which was precisely polished with a surface roughness less than 2 nm. The subsurface structure of specimens was examined using cross-sectional transmission electron microscopy (XTEM) to guarantee that the specimens were damage-free before testing. The indentations were conducted on a nano-Triboindenter (Hysitron Inc., USA) using a Berkovich indenter in ambient conditions. The maximum loads varied from 100 μN to 30 mN whereas the loading rates ranged from 5 μN/s to 10 mN/s. The holding time at the maximum loads for all the tests was 30 s to minimize the time-dependent plastic effect. For each condition, at least 16 tests were repeated.

Conventional TEM studies were carried out in a Philips CM12 transmission electron microscope, operating at 120 kV. The TEM specimens were prepared by a technique using a tripod [19]. In the preparation, the material removal was continuously monitored and the sample position with respect to the tripod was adjusted during the mechanical thinning. Finally, ion-beam thinning was carried out to provide a sufficiently thin area for the TEM investigations.

3. Results and discussion

3.1. Mechanical characterisation of silicon using nanoindentation

Prior to indentation, the area function of the indenter tip was measured in a fused quartz, a standard material for this purpose [20]. The experimental data are shown in Fig. 1 and fitted by equation [20]

$$A = C_0h_c^2 + C_1h_c + C_2h_c^{1/2} + \cdots + C_8h_c^{1/128} \quad (1)$$

where h_c is the contact depth and A is the nominal contact area. C_1 through C_8 are constants. It was found that when the contact depth is less than 20 nm, the indenter can be described as a spherical tip with the form of $A = 2\pi Rh_c$, where R is the radius of the indenter tip. In our case, the tip radius $R = 227$ nm is obtained from the fitted equation. When the contact depth is deeper than 500 nm, the indenter can be treated as a perfect Bekovich indenter ($A = 24.5h_c$). However, when the contact depth is between these values, the indenter needs to be described by $A = a_1h_c^2 + a_2h_c$, where the first term represents the pyramidal indenter and the second describes a spherical one [20]. The results show that the Berkovich indenter is not perfectly sharp but with a spherical tip. Hence, different area functions should be used for data analysis on the basis of the real contact depth in indentation tests.

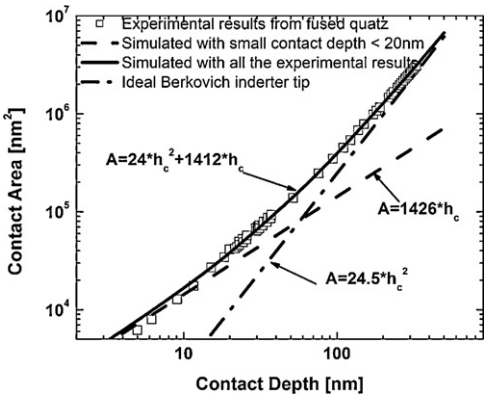

Fig. 1. The measured area function of the indenter tip.

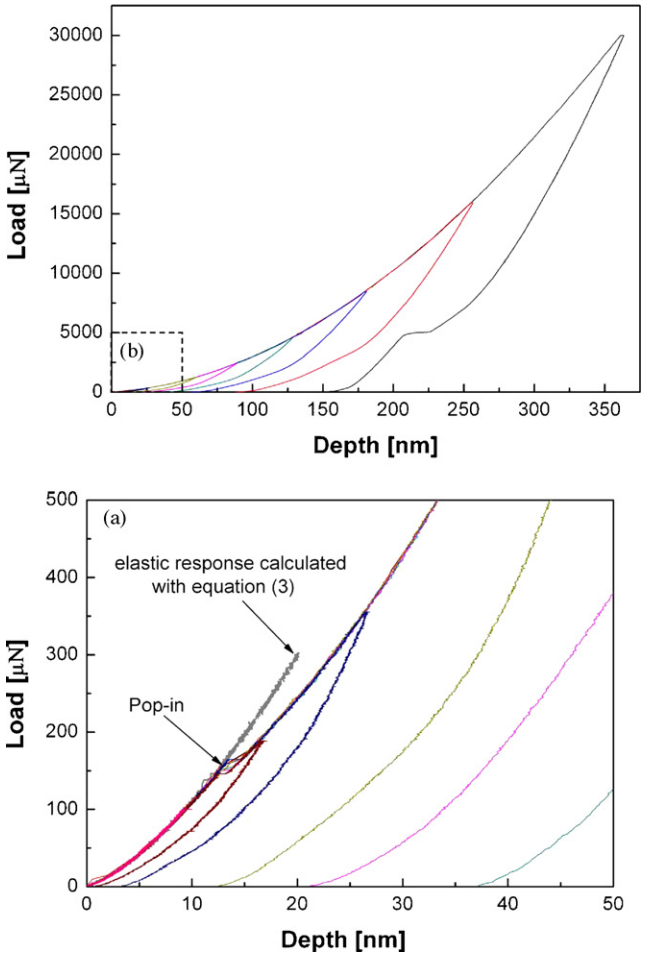

Fig. 2. (a) The load–depth curves measured under different loading conditions and (b) a magnified view under ultra-low loads. The peak loads are varied in the range of 100 μN to 30 mN, while the duration of the loading and unloading processes was kept the same, 30 s.

With the contact area defined above, the mechanical properties of silicon can be accurately characterised under different loading conditions. Fig. 2(a) shows the load–displacement curves with different maximum loads (P_{max}) having different loading/unloading rates. Fig. 2(b) is a magnified view for Fig. 2(a) under ultra-low loads, in which "pop-in" can be clearly observed. As shown in the figure, when the maximum load varied from 200 μN to 30 mN the measured hardness (H) of silicon and the reduced Young's modulus of the indentation system (E_r) are $H = 12.7 \pm 0.5$ GPa and $E_r = 160 \pm 4.2$ GPa. Then, the Young's modulus of silicon can be determined to be $E_s = 171$ GPa, according to contact mechanics [21]

$$\frac{1}{E_r} = \frac{1-\nu_d^2}{E_d} + \frac{1-\nu_s^2}{E_s} \quad (2)$$

where $E_d = 1050$ GPa is the Young's modulus of the Berkovich diamond indenter, and $\nu_d = 0.10$ and $\nu_s = 0.28$ are the Poisson's ratios of

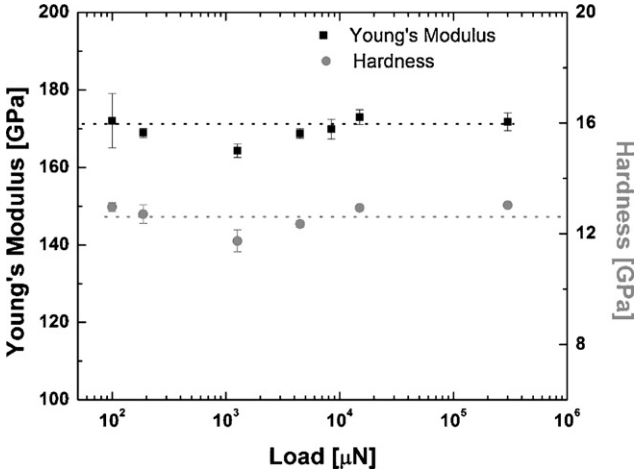

Fig. 3. Hardness and Young's modulus of silicon as a function of indent depth measured with various peak loads having different loading/unloading rates. The load–displacement curves and loading conditions are given in Fig. 2.

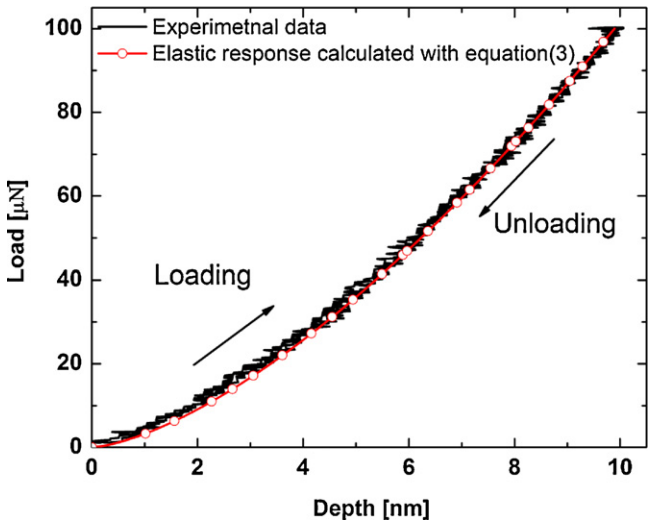

Fig. 4. Elastic deformation in silicon when the maximum indentation load is below 100 μN.

the indenter and silicon [22]. The measured values of hardness and modulus are summarized in Fig. 3 as a function of indent depth. It is interesting to note that both E_s and H are almost constant even when the indentation depth varies in a wide range, from 10 nm to 300 nm. However, it is well known that nanoindentation tests sometime show size-effect, i.e. the increase of hardness with the decrease of indentation depth. There are two major factors account for such size-effect: (1) geometrically necessary dislocations (GNDs) underneath an indenter tip [23] and (2) underestimation of the contact area by treating indenter as a perfectly sharp one [24]. However, under nanoindentation, the plastic deformation in silicon is solely caused by phase transformation rather than the dislocation of crystal lattice and thus GNDs model is invalid here. Therefore, once the indenter tip can be accurately described, the hardness and modulus of silicon measured by nanoindentation could be stable, without the size-effect (Fig. 3). The constant elastic modulus measured over a wide range of loading conditions indicates that high-pressure phases of silicon formed during loading have a negligible effect on the elasticity of the material at the initial unloading. This is because the high-pressure phases are stable during the initial unloading process and therefore the overall elastic response of the material is governed by the elastic property of the Si-I phase. As a result, the modulus of silicon can be accurately measured in this way.

Fig. 4 demonstrates that silicon is perfectly elastic up to the maximum indentation load of 100 μN. This is well supported by the cross-sectional TEM examination after the indentation test (Fig. 5), which shows that the subsurface structure of the specimen is damage-free, and hence the deformation during indentation was truly elastic. Since the indentation depth is less than 20 nm under the present loading condition, the indenter is considered as spherical (Fig. 1). According to the Hertz contact theory, the ideal elastic response of silicon is described by [21],

$$P = \frac{4}{3} E_r R^{1/2} h_t^{3/2} \tag{3}$$

where P is the load and h_t is the indentation depth. The values of E_r and R are experimentally determined as discussed above. The excellent agreement between experiment and theory well justifies that the Young's modulus we determined is very accurate.

3.2. Pop-in behaviour of silicon and effect of stressing

As shown in Fig. 2(b), the pop-in occurs on the load–displacement curves, associated with the transition from purely elastic to elastic/plastic deformation. To further examine pop-in behaviour of silicon and the stressing effect, we conducted indentations at the load of 300 μN with different loading rates and results are presented in Fig. 6. As shown in the figure, under a relatively higher loading rate (30 μN/s), the slope of displacement curve gradually changes without apparent pop-in discontinuity. With slower loading process, e.g. 10 μN/s, pop-in occurs. The pop-in events show reasonable repeatability. It is also noticed that pop-in always represents the transition from purely elastic deformation to elastic–plastic deformation, suggesting the onset of phase transition. According to contact mechanics, the contact pressure during loading can be calculated as a function of the indentation depth/load [25]. As shown in Fig. 7, the critical contact pressure at the onset of inelastic deformation is about 15 GPa. This is consistent with the theoretical value of the contact pressure 14.3 GPa in order to induce Si-I to Si-II phase transition under spherical indentations [26]. Hence, our result does show that inelastic deformation in silicon under nanoindentation is due to the phase transition. At a glance, it does not seem to be straightforward that the hardness can remain unchanged over a wide range of the indentation

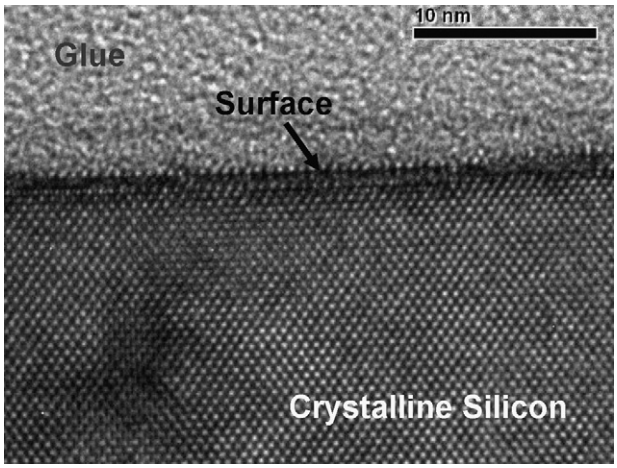

Fig. 5. Subsurface microstructure of silicon after the indentation test with a peak load of 100 μN.

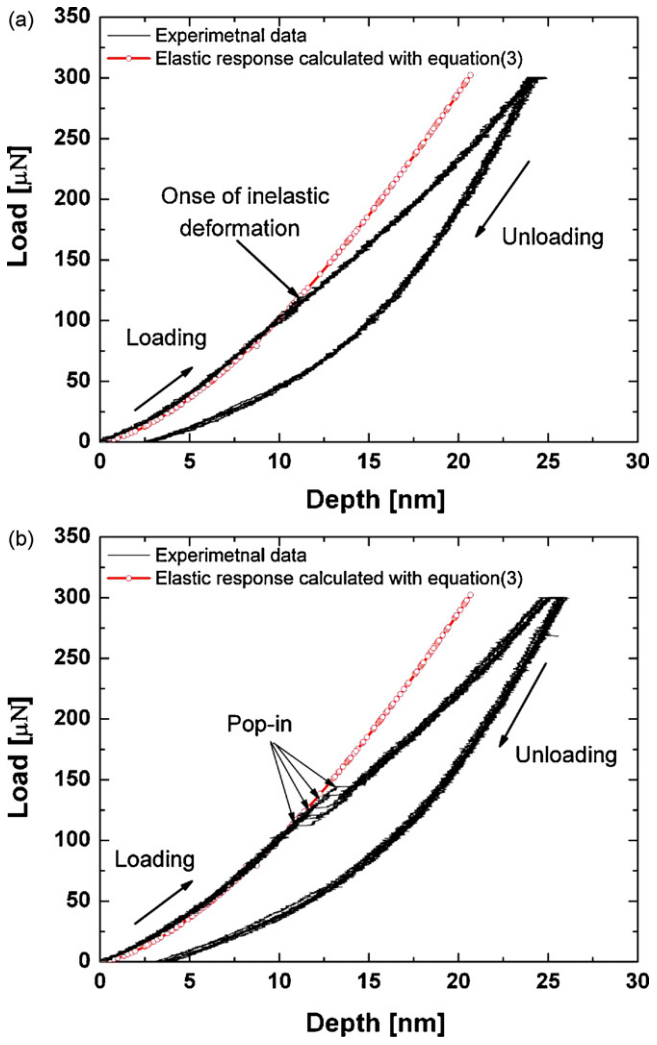

Fig. 6. Load–displacement curves: (a) maximum load of 300 μN with the loading/unloading rate of 10 μN/s and (b) maximum load of 300 μN with the loading/unloading rate of 30 μN/s.

loads tested. It becomes clear if we recall that the hardness is the material's resistance to plastic deformation loaded by an indenter. The hardness value of a material is determined by the average contact pressure when the material responds plastically. If a material has a plastic hardening behaviour, its hardness will change as the indentation load varies. In the case of silicon, however, the material behaves perfectly plastically when phase transformation takes place, i.e. no hardening as shown in Fig. 7; thus the hardness remains a constant. This is in agreement with our earlier conclusion.

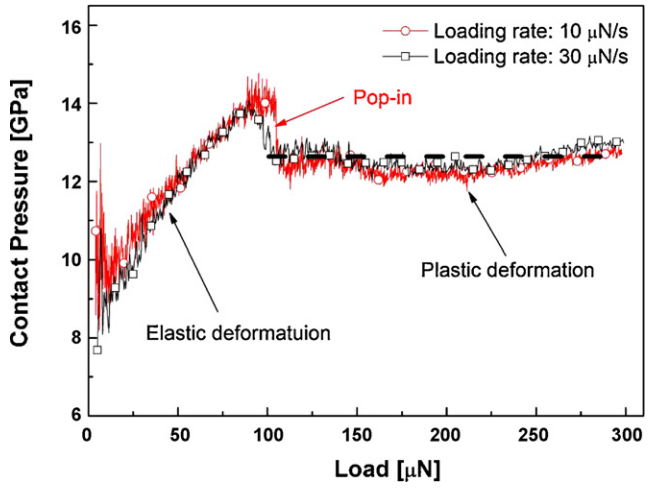

Fig. 7. The contact pressure as a function of displacement for the loading–displacement curves with and without pop-in event.

It is evident that the shape of the load–displacement curves is significantly influenced by loading rate. In our case, at the highest loading rate of 30 μN/s, none of the 16 tests yielded any detectable pop-in (Fig. 6a). With an intermediate loading rate of 15 μN/s, 5 of the 16 tests gave pop-ins, but the rest produced only gradual slope changes. At a slower loading process (5 μN/s and 10 μN/s), pop-in always occurred (Fig. 6b). The results also explain why some researchers [27] could not observe pop-ins using a Berkovich indenter with the loading rates from 0.2 mN/s to 40 mN/s, as the rates were too high for a pop-in to take place. The above experimental results show that a low loading rate favors pop-in, i.e. the distinct displacement discontinuity/jump in the loading curve. Such a sudden displacement jump suggests that a rapid volume shrinkage in the indentation-induced deformation zone is taking place at the pop-in, which should correspond to a phase change from the Si-I phase to the more dense Si-II phase [13–15]. Since a crystalline growth like this requires a time span to generate sufficient nucleation sites and to allow the crystalline to grow to a certain volume, it is understandable that the occurrence of a pop-in is associated with a slow loading rate. The variation of the locations of the pop-ins (Fig. 6b) can be caused by the small perturbation of indentation conditions such as a thermal drift, which is more influential to an indentation at a slower loading rate, and surface roughness, which can alter the local stress distribution in the neighborhood of the indentation zone and in turn affect the process of the crystalline growth. With a fast loading rate, however, once the contact pressure reaches the critical value, phase transition initiates at the place of the highest stress and expands to its surrounding area. A sudden volume shrinkage cannot happen, and as such the slope of the load–displacement curve only varies gradually (Fig. 6a).

Therefore, repeatable pop-in events occurring under ultra-low loading represent the onset of phase transition, resulting in inelastic deformation in silicon. This is different from that pop-in behaviour observed in spherical indentations under relatively high loads, e.g. >50 mN [1,10]. In that case, the position of the pop-ins shows little repeatability, which could be caused by phase transformation, subsurface cracking, or sudden dislocation bursts [10]. Further, because material behaviour is governed by plastic deformation under such high loads, the contact pressure for "pop-in" is actually the measured hardness and cannot be considered as the critical pressure for the onset of phase transition under indentation.

4. Conclusion

In summary, based on our investigation into the deformation behaviour of silicon under ultra-low loading conditions with nanoindentation using a Berkovich indenter, we found that with a proper area function of the indenter tip the mechanical properties of silicon can be accurately characterised. The measured Young's modulus of silicon (1 0 0) is 171 GPa. The material is perfectly elastic up to the maximum indentation load of 100 μN. The pop-in on a load–displacement curve represents the onset of the phase transition from Si-I to Si-II. The shape of a loading curve is influenced by loading rate. A lower rate favors a sudden volume change, and hence pop-in occurs; whereas a rapid loading process tends to generate a gradual slope change on the curve.

Acknowledgement

The authors appreciate the financial support of the Australian Research Council.

References

[1] E.R. Weppelmann, J.S. Field, M.V. Swain, J. Mater. Sci. 30 (1995) 2455.
[2] A. Kailer, Y.G. Gogotsi, K.G. Nickel, J. Appl. Phys. 87 (1997) 3057.
[3] I. Zarudi, L.C. Zhang, Tribol. Int. 32 (1999) 701.
[4] J.E. Bradby, J.S. Williams, J. Wong-Leung, M.V. Swain, P. Munroe, Appl. Phys. Lett. 77 (2000) 3749.
[5] X.D. Li, B. Bhushan, K. Takashima, C.W. Baek, Y.K. Kim, Ultramicroscopy 97 (2003) 481.
[6] T.H. Fang, W.J. Chang, C.M. Lin, Microelectron. Eng. 77 (2005) 389.
[7] T. Vodenitcharova, L.C. Zhang, Int. J. Solids Struct. 40 (2003) 2989.
[8] S.W. Youn, C.G. Kang, Mater. Sci. Eng. A 390 (2005) 233.
[9] M. Yoshino, T. Aoki, N. Chandrasekaran, T. Shirakashi, R. Komanduri, Int. J. Mech. Sci. 43 (2001) 313.
[10] T. Juliano, V. Domnich, Y. Gogotsi, J. Mater. Res. 19 (2004) 3099.
[11] J.Z. Hu, L.D. Merkle, C.S. Menoni, I.L. Spain, Phys. Rev. B 34 (1986) 4679.
[12] W.C.D. Cheong, L.C. Zhang, J. Mater. Sci. Lett. 19 (2000) 439.
[13] L.C. Zhang, H. Tanaka, JSME Int. J. Ser. A 31 (1999) 546.
[14] W.C.D. Cheong, L.C. Zhang, Nanotechnology 11 (2000) 173.
[15] K. Mylvaganam, L.C. Zhang, P. Eyben, J. Mody, W. Vandervorst, Acta Mater., in press.
[16] H.S. Leipner, D. Lorenz, A. Zeckzer, H. Lei, P. Grau, Phys. B 308–310 (2001) 446.
[17] D. Lorenz, A. Zeckzer, U. Hilpert, P. Grau, H. Johansen, H.S. Leipner, Phys. Rev. B 67 (2003) 172101.
[18] I. Zarudi, J. Zou, L.C. Zhang, Appl. Phys. Lett. 82 (2003) 874.
[19] I. Zarudi, L.C. Zhang, J. Mater. Process. Technol. 84 (1998) 149.
[20] H. Bei, E.P. George, J.L. Hay, G.M. Pharr, Phys. Rev. Lett. 95 (2005) 045501.
[21] K.L. Johnson, Contact Mechanics, Cambridge University Press, New York, 1985.
[22] C.T. Lynch, CRC Handbook of Materials Science, 4th ed., CRC Press, Boca Raton, 1986.
[23] W.D. Nix, H. Gao, J. Mech. Phys. Solids 46 (1998) 411–425.
[24] S. Qu, Y. Huang, W.D. Nix, H. Jiang, F. Zhang, K.C. Hwang, J. Mater. Res. 19 (2004) 3423–3434.
[25] L. Chang, L.C. Zhang, Modern Phys. Lett. B, in press.
[26] M. Hebbache, M. Zemzemi, Phys. Rev. B 67 (2003) 233302.
[27] J.W. Yan, H.T. Takahashi, X.H. Gai, H. Harada, J. Tamaki, T. Kuriyagawa, Mater. Sci. Eng. A 423 (2006) 19.